

# A Density Functional Theory Study on Electronic Structure and Second-order Nonlinear Optical Properties of Some Push-Pull Molecules

SA, Rong-Jian(洒荣建) · WU, Ke-Chen\* (吴克琛) LIN, Chen-Sheng(林晨升) LIU, Ping(刘萍)  
MANG, Chao-Yong(莽朝永)

State Key Laboratory of Structural Chemistry, Fujian Institute of Research on the Structure of Matter, Chinese Academy of Sciences, Fuzhou, Fujian 350002, China

Time-dependent density-functional theory (TDDFT) has been applied to calculate the electronic structure and second-order nonlinear optical (NLO) properties of some organic molecules. The two-dimensional (2-D) charge transfer characteristics of calculated molecules were studied and compared with corresponding experimental results. All the theoretical results agree well with the measurement. For 2-D molecule with two-fold symmetry, the dominant charge transfer is off-diagonal, while for three-fold symmetry 2-D molecule, the dominant charge transfer is not only between branches and central group but also among branches.

**Keywords** TDDFT, electronic absorption spectra, second-order NLO property, 2-D charge transfer

## Introduction

The exploring of new nonlinear optical (NLO) materials has attracted much attention during the past three decades because of their potential application in optoelectronic and optical signal processing. Organic crystals have been studied widely since 1970s due to their favorable features for second harmonic generation (SHG) and related applications. Compared with inorganic molecules, organic molecules offer a high molecular hyperpolarizability, fast response time, facile structural modification and relative ease of device processing.<sup>1-3</sup>

The typical organic molecules designed for large  $\beta$  values generally possess conjugated  $\pi$ -systems with donor-acceptor pair such as *p*-nitroaniline (PNA) like compounds.<sup>1-3</sup> The largest components of  $\beta$  are parallel to the dipole direction, and the charge transfer (CT) along the dipole direction is one-dimensional (1-D). To understand the structure-property relationship in the molecule, a great deal of studies has been carried out over the past two decades; both experimental based on electric field induced second-harmonic generation in solution (EFISH)<sup>4</sup> and theoretical approach based on "two-level model" are included.<sup>1</sup> More recently, there are many reports on the NLO molecules with 2-D CT based on 1-D CT

system,<sup>1,3,5</sup> and the most common examples of 2-D molecule are (dicyanomethylene)pyran (DADB) and trinitrotriaminobenzene (TATB). Compared with 1-D CT molecules, there are large off-diagonal tensors of  $\beta$  in 2-D NLO molecules. It was also reported that 2-D CT can be used to arrange the contradiction among nonlinearity efficiency, transparency and thermal stability of NLO materials.<sup>3,5,6</sup>

To understand the structure-property relationships of 2-D molecules, some computational chemistry studies based on "multipolar theory"<sup>1</sup> were reported. It is recognized that to compare with experimental measurement directly, frequent dependency should be considered in the calculation. However, most of the reported calculations on 2-D molecule with frequency dependency are based on semi-empirical method.<sup>1</sup> Thus more accurate calculation with frequency dependency is expected. In this paper, we chose some organic NLO molecules which have been characterized by Wolff and Wortman<sup>3,6</sup> (Fig. 1). Fig. 2 shows the sketch of selected molecule 1. Their structure-property relationships were studied by a time-dependent density-functional theory (TDDFT)<sup>7-9</sup> calculation. All results show good agreement with experimental measurement.

## Methods and computational details

Structural optimizations have been performed on all molecules. According to the experimental results, we assumed  $C_{2v}$  symmetry for molecules 1—5 and  $D_{3h}$  symmetry for molecules 6—7. The representative optimized results of molecule 1 are listed in Table 1. The second-order polarizabilities were calculated by the TDDFT<sup>7-9</sup> approach. For structural optimization calculations, the generalized gradient approximation (GGA) exchange-correlation (XC) potential based on the Becke-Perdew<sup>10</sup> approximation was applied. For second-order polarizability calculation, the LB94<sup>11</sup> XC potentials which adopted the asymptotic behavior correction were

\* E-mail: wkc@ms.fjirsm.ac.cn; Fax: +86-591-3714946

Received July 11, 2002; revised November 14, 2002; accepted December 2, 2002.

Project supported by the National Natural Science Foundation of China (Nos. 69978021 and 20173064) and the Fujian Provincial Natural Science Foundation of China (No. E9910030).

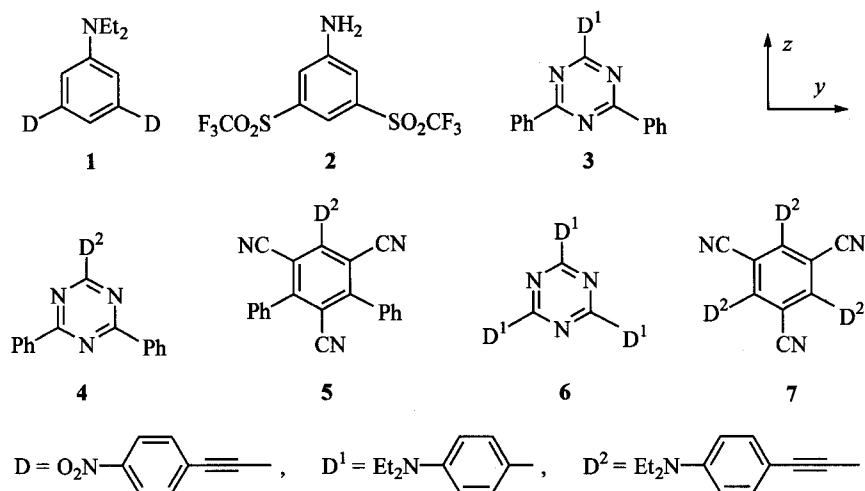


Fig. 1 Molecular structures and orientation of calculated molecules.

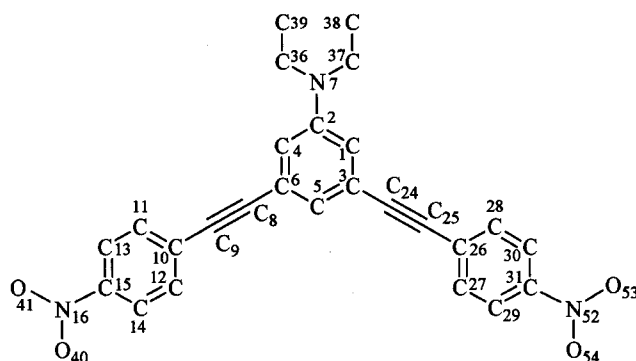


Fig. 2 Sketch of selected molecule 1.

Table 1 Optimized bond length (nm) and bond angle (°) in molecule 1

C(1)—C(2)/C(2)—C(4)	0.1414	C(1)—C(3)/C(4)—C(6)	0.1402
C(3)—C(5)/C(5)—C(6)	0.1399	C(8)—C(9)/C(24)—C(25)	0.1216
C(6)—C(8)/C(3)—C(24)	0.1413	C(9)—C(10)/C(25)—C(26)	0.1409
C(10)—C(11)/C(26)—C(28)	0.1409	C(10)—C(12)/C(26)—C(27)	0.1411
C(11)—C(13)/C(30)—C(31)	0.1383	C(13)—C(15)/C(30)—C(31)	0.1391
C(14)—C(15)/C(29)—C(31)	0.1402	C(15)—N(16)/C(31)—N(52)	0.1458
N(16)—O(41)/N(52)—O(53)	0.1239	N(16)—O(40)/N(52)—O(54)	0.1237
C(2)—N(7)	0.1382	C(37)—C(38)/C(36)—C(39)	0.1523
C(2)—C(1)—C(3)/C(2)—C(4)—C(6)	121.5	C(1)—C(2)—C(4)	116.8
C(4)—C(6)—C(5)/C(1)—C(3)—C(5)	120.9	C(3)—C(5)—C(6)	118.5
C(2)—N(7)—C(36)/C(2)—N(7)—C(37)	115.5	N(7)—C(36)—C(39)/N(7)—C(37)—C(38)	120.6
C(6)—C(8)—C(9)/C(3)—C(24)—C(25) *	178.6	C(11)—C(10)—C(12)/C(27)—C(26)—C(28)	119.3
C(10)—C(11)—C(13)/C(26)—C(28)—C(30)	120.6	C(11)—C(13)—C(15)/C(28)—C(30)—C(31)	118.6
C(13)—C(15)—C(14)/C(30)—C(31)—C(29)	122.1	C(15)—C(14)—C(12)/C(31)—C(29)—C(27)	118.5
O(41)—N(16)—O(40)/O(53)—N(52)—O(54)	125.3	C(15)—N(16)—O(41)/C(31)—N(52)—O(53)	116.7

utilized. There are some recent reports indicating that LB94 can achieve more accurate results for hyperpolarizability calculations than other XC approximations. We use the standard ADF III basis set for the calculations, which is a double- $\xi$  STO basis set with one polarization function added. The cores (C, O, N, F: 1s, S: 2p) were kept frozen. All the struc-

tural optimization and polarizability calculations reported in this paper were performed at ADF 2000<sup>12</sup> package.

Electronic absorption spectra of the chosen molecules were calculated by the TDDFT calculation implemented in the Gaussian98w package.<sup>13</sup> The method utilized is the three-parameter hybrid functional according to Becke with additional

correlations due to Lee *et al.*<sup>14,15</sup> (B3LYP), with standard Gaussian 6-31G basis set. Molecular coordinates were taken from the ADF optimized results.

### Ground and excited electronic structures

The first 30 lowest singlet excited states of molecule 1 and molecule 6 were calculated. Tables 2 and 3 list the dominant excited states of molecules 1 and 6. Fig. 3 shows the molecular orbitals of 1 and 6. Fig. 4 is the electronic absorp-

tion spectra of the two molecules.

From Table 2, we can find the HOMO orbital is not direct contribution to the seven main transitions of molecule 1. HOMO - 1, LUMO and LUMO + 1 orbitals of molecule 1 (shown in Fig. 3) are mainly composed of the two branch groups and central phenyl, but there are some differences among them. For HOMO - 1 orbital, the central phenyl contributes more than other two molecular orbitals. For other frontier orbitals of molecule 1, HOMO - 2, LUMO + 2 and LUMO + 3, the main difference is the NEt<sub>2</sub> group. For LUMO + 2

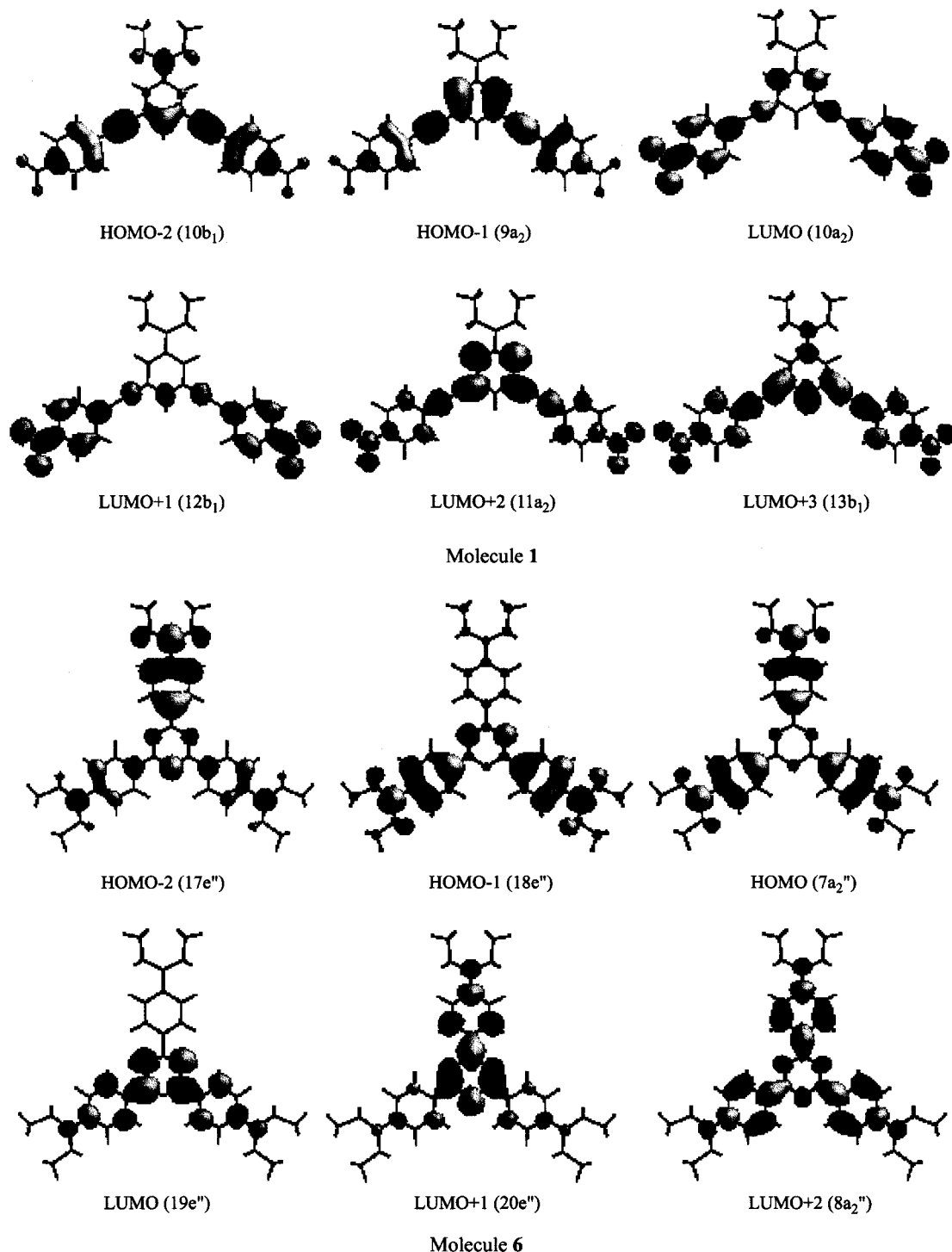


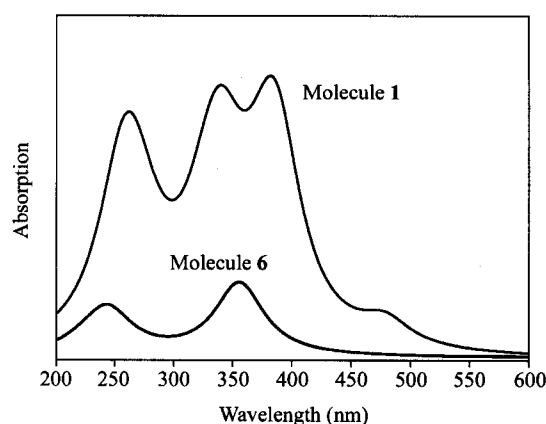
Fig. 3 Molecular orbitals of molecules 1 and 6.

**Table 2** Dominant TD/B3LYP vertical excitation energy ( $\lambda$ , nm), the corresponding oscillator strength ( $f$ ) and configurations for molecule **1**

State	Theory		Expt	Composition
	$\lambda$	$f$		
$2^1B_2$	387.0	0.6743	393	0.68 ( $9a_2 \rightarrow 12b_1$ )
$2^1A_1$	376.2	0.2072		0.67 ( $9a_2 \rightarrow 10a_2$ )
$3^1B_2$	340.1	0.5690	322	0.68 ( $10b_1 \rightarrow 10a_2$ )
$3^1A_1$	327.4	0.1911		0.67 ( $10b_1 \rightarrow 12b_1$ )
$6^1A_1$	269.0	0.2441		0.64 ( $9a_2 \rightarrow 11a_2$ )
$7^1B_2$	259.5	0.3580		0.66 ( $9a_2 \rightarrow 13b_1$ )
$8^1B_2$	254.6	0.2201		0.67 ( $10b_1 \rightarrow 11a_2$ )

**Table 3** Dominant TD/B3LYP vertical excitation energy ( $\lambda$ , nm), the corresponding oscillator strength ( $f$ ) and configurations for molecule **6**

State	Theory		Expt	Composition
	$\lambda$	$f$		
$21E''$	354.5	0.1037	373	0.42 ( $18e'' \rightarrow 19e''$ ) + 0.27 ( $7a_2'' \rightarrow 19e''$ ) - 0.42 ( $17e'' \rightarrow 20e''$ )
$31E''$	354.5	0.1037		0.42 ( $17e'' \rightarrow 19e''$ ) + 0.42 ( $18e'' \rightarrow 20e''$ ) - 0.27 ( $7a_2'' \rightarrow 19e''$ )
$91E'$	243.3	0.0660		0.49 ( $17e'' \rightarrow 8a_2''$ ) + 0.35 ( $18e'' \rightarrow 8a_2''$ )
$101E'$	243.3	0.0660		0.49 ( $18e'' \rightarrow 8a_2''$ ) - 0.35 ( $17e'' \rightarrow 8a_2''$ )

**Fig. 4** Calculated electronic absorption spectra of molecules **1** and **6**.

orbital,  $NEt_2$  group shows little contribution. Three main absorption bands of molecule **1** are shown in Fig. 4, and the maximum absorption band, located at  $\sim 387$  nm, is mainly formed by the excitation state  $2^1B_2$ , which mainly denotes a HOMO - 1  $\rightarrow$  LUMO + 1 transition. We assign the maximum absorption of molecule **1** as the charge transfer from central group to branch groups. The second absorption band located at  $\sim 340$  nm is mainly formed by  $3^1B_2$ . The dominant configuration of  $3^1B_2$  is HOMO - 2  $\rightarrow$  LUMO. Comparing the middle absorption band with the maximum absorption band, there

are more contributions of  $NEt_2$  groups in HOMO - 2 orbital than in the HOMO - 1 orbital. The minimum absorption band of molecule **1** is located at  $\sim 259$  nm, which denotes a UV absorption. And the corresponding transition is  $7^1B_2$ . The dominant transition of  $7^1B_2$  is HOMO - 1  $\rightarrow$  LUMO + 3. The strongest excitation states of molecule **1** are  $2^1B_2$  and  $3^1B_2$ , and the dominant charge transfer of them is along the two branch groups. So the off-diagonal directions show more feasible charge transfer than the diagonal direction.

To molecule **6**, there are only HOMO and LUMO + 2 orbitals showing three-fold symmetry, while the other frontier orbitals show two-fold symmetry. Two main absorption bands in the absorption spectra are found. The maximum absorption band is two degenerated excited states  $2^1E''$  and  $3^1E''$ . The dominant configurations of the two states are the combination of HOMO - 1  $\rightarrow$  LUMO + 1, HOMO  $\rightarrow$  LUMO + 1 and HOMO - 2  $\rightarrow$  LUMO + 2. HOMO - 1  $\rightarrow$  LUMO + 1 is the transition among the three branch groups, from two branch groups to another branch group. HOMO  $\rightarrow$  LUMO + 1 is the transition among the three branch groups and central aromatic ring. While the HOMO - 2  $\rightarrow$  LUMO + 2 transition is mainly from one branch group to the other two branches. The other absorption band located at *ca.* 243 nm, is mainly formed by two degenerated excited states  $9^1E'$  and  $10^1E'$ . Their dominant transitions are HOMO - 1  $\rightarrow$  LUMO + 2 and HOMO - 2  $\rightarrow$  LUMO + 2. The HOMO - 1  $\rightarrow$  LUMO + 2 is the transition from two branch groups to another branch group and the transition of HOMO - 2  $\rightarrow$  LUMO + 2 is from one branch group to the other two branches.

### Calculated second-order NLO properties

According to "three-level model",<sup>1</sup> the nonzero  $\beta$  tensor of  $C_{2v}$  molecules will be seven independent components:  $\beta_{xxx} = \beta_{xxx}$ ,  $\beta_{yyz} = \beta_{zyy}$ ,  $\beta_{zxx}$ ,  $\beta_{zzz}$  and  $\beta_{zyy}$ , and only three independent components  $\beta_{yyz} = \beta_{zyy}$ ,  $\beta_{zzz}$  and  $\beta_{zyy}$ , are dominant. For  $D_{3h}$  symmetry molecules, there are four significant components  $\beta_{zzz} = -\beta_{zyy} = -\beta_{yyz} = -\beta_{zyy}$ . Here, the  $z$  direction is the dipole moment direction of the calculated molecules. The calculated results and corresponding experimental data are listed in Tables 4 and 5.

From the Table 4 and Table 5, the calculated values agree with experimental results well. All the molecules show large  $\beta$  values except for molecule **2**. Molecule **1** and molecule **2** show larger off-diagonal components of  $\beta$  ( $\beta_{zyy}$ ,  $\beta_{yyz}$  and  $\beta_{zyy}$ ) than the diagonal component  $\beta_{zzz}$ . Molecule **2** has a strong acceptor group ( $-SO_2CF_3$ ), and shows large dipole moment. But its  $\beta$  values are small due to the lack of conjugate effect. The contributions of conjugation to  $\beta$  values in these molecules are larger than simple push-pull interaction. The geometry of molecule **3** is similar to that of molecule **4**, and the difference of  $\beta$  values ( $4 > 3$ ) may come from the length of conjugation pairs. Thus the additional conjugation length is favorable to  $\beta$ . For molecules **6** and **7**, off-diagonal components of  $\beta$  are equal to the diagonal ones due

**Table 4** Experimental and calculated NLO properties for molecules 1—7 (unit:  $10^{-30}$  esu)

	$\mu$ (D)		$\beta_{1.064}$	
	Calcd	Expt	Calcd	Expt
1	10.3	$8.0 \pm 0.1$	31	$43 \pm 11$
2	11.2	$6.0 \pm 0.3$	4.8	$4.8 \pm 0.5(\beta_z)$
3	4.8	3.3	323	259
4	6.7	3.6	1211	447
5	4.8	4.2	4027	4095
6	0	—	313	383
7	0	—	4197	7220

Experimental data of molecules 1 and 2 come from Ref. 3 and Ref. 6 obtained by HRS. Both experimental and calculated values are performed at  $\lambda = 1.064 \mu\text{m}$ .  $\beta = \beta_{zz}$  for molecules 1—4 with the z-axis is the direction of dipole moment.  $\beta = \beta_{zz} = -\beta_{yy} = -\beta_{yz} = -\beta_{xy}$  for 6 and 7.  $\beta_z$  for 2 obtained by EFISH measurement performed at  $\lambda = 1.064 \mu\text{m}$ , corresponding value:  $\beta_z = \beta_{zz} + \beta_{yy}$ .<sup>1</sup> And all calculated values of  $\beta$  are absolute ones.

**Table 5** Calculated  $\beta$  components of molecules 1—5 (unit:  $10^{-30}$  esu)

	$\beta_{zz}$		$\beta_{yy}$		$\beta_{yz}$	
	Calcd	Expt	Calcd	Expt	Calcd	Expt
1	31	$43 \pm 11$	176	$181 \pm 11$	569	$194 \pm 23$
2	1.8	—	3.0	—	1.5	—
3	323	259	30	—	56	—
4	447	1211	55	—	29	—
5	4027	4095	157	—	63	—

to the  $D_{3h}$  symmetry, and components of 7 are larger than those of 6 because the corresponding pushing and pulling electron abilities of 7 are stronger than those of 6. In conclusion, molecules 1, 2, 6 and 7 show a clear 2-D CT properties while other molecules show 1-D CT character. The  $\beta$  values of some calculated 2-D molecules are comparable with those of 1-D molecule. But their large off-diagonal  $\beta$  values may be useful to design new NLO materials with large  $\beta$  values. The 2-D molecules contain more donors and acceptors than 1-D molecules, so the structural modification may be feasible.

## Conclusions

In this paper, the electronic absorption spectra of selected molecules have been studied using TDDFT method. The calculation results indicate that the off-diagonal charge transfer of 2-D molecules is dominant. The frequency-dependent  $\beta$  was calculated by TDDFT theory with accurate LB94 XC potentials. The 2-D properties of the molecules were studied and compared with corresponding HRS measurement. The calculation showed that 2-D molecule contains favorable electronic transition and flexible structural modification. TDDFT calculation provides a powerful and efficient tool to

study the electronic spectra and second-order NLO properties of 2-D molecules.

## Acknowledgement

One of the authors SA, Rong-Jian is grateful to the kind help of Prof. Wortmann, R. and Prof. Goovaerts, E.

## References

- Zyss, J.; Ledoux, I. *Chem. Rev.* **1994**, *94*, 77.
- Samuel, D. W.; Dhenaut, C.; Ledoux, I.; Zyss, J.; Bourgaud, M.; Le Bozec, H. *Nature* **1995**, *374*, 339.
- Wolff, J. J.; Längle, D.; Hillenbrand, D.; Wortmann, R.; Matschiner, R.; Glania, C.; Krämer, P. *Adv. Mater.* **1997**, *9*, 138.
- Qudar, J. L. *J. Chem. Phys.* **1977**, *67*, 446.
- Moylan, C. R.; Emmer, S.; Lovejoy, S. M.; McComb, I. H.; Leuny, D. S.; Wortmann, R.; Kramer, P.; Twieg, R. J. *J. Am. Chem. Soc.* **1996**, *118*, 12950.
- Wolff, J. J.; Siegler, F.; Matschiner, R.; Wortmann, R. *Angew. Chem., Int. Ed.* **2000**, *39*, 1436.
- Champagne, B.; Perpete, E. A.; van Gisbergen, S. J. A.; Baerends, E. J.; Sniijders, J. G.; Soibra-Ghaoui, C.; Robins, K.; Kirtman, B. *J. Chem. Phys.* **1998**, *109*, 10657.
- Ricciardi, G.; Rosa, A.; van Gisbergen, S. J. A.; Baerends, E. J. *J. Phys. Chem. A* **2000**, *104*, 635.
- van Gisbergen, S. J. A.; Sniijders, J. G.; Baerends, E. J. *Comput. Phys. Commun.* **1999**, *118*, 119.
- (a) Becke, A. D. *Phys. Rev. A* **1988**, *38*, 3098.  
(b) Perdew, J. P.; Wang, Y. *Phys. Rev. B* **1986**, *33*, 8800.
- van Leeuwen, R.; Baerends, E. J. *Phys. Rev. A* **1994**, *49*, 2421.
- Fonseca Guerra, C.; Sniijders, J. G.; te Velde, G.; Baerends, E. J. *Theor. Chem. Acc.* **1998**, *99*, 391.
- Frisch, M. J.; Trucks, G. W.; Schlegel, H. B.; Scuseria, G. E.; Robb, M. A.; Cheeseman, J. R.; Zakrzewski, V. G.; Montgomery, J. A.; Stratmann, R. E.; Burant, J. C.; Dapprich, S.; Millam, J. M.; Daniels, A. D.; Kudin, K. N.; Strain, M. C.; Farkas, O.; Tomasi, J.; Barone, V.; Cossi, M.; Cammi, R.; Mennucci, B.; Pomelli, C.; Adamo, C.; Clifford, S.; Ochterski, J.; Petersson, G. A.; Ayala, P.; Y.; Cui, Q.; Morokuma, K.; Salvador, P.; Dannenberg, J. J.; Malick, D. K.; Rabuck, A. D.; Raghavachari, K.; Foresman, J. B.; Cioslowski, J.; Ortiz, J. V.; Baboul, A. G.; Stefanov, B. B.; Liu, G.; Liashenko, A.; Piskorz, P.; Komaromi, I.; Gomperts, R.; Martin, R. L.; Fox, D. J.; Keith, T.; Al-Laham, M.; A.; Peng, C. Y.; Nanayakkara, A.; Challacombe, M.; Gill, P. M. W.; Johnson, B.; Chen, W.; Wong, M. W.; Andres, J. L.; Gonzalez, C.; Head-Gordon, M.; Replogle, E. S.; Pople, J. A. *Gaussian 98* (Revision A.7), Gaussian, Inc., Pittsburgh PA, **1998**.
- Lee, C.; Yang, W.; Parr, R. G. *Phys. Rev. B* **1988**, *37*, 785.
- Becke, A. D. *J. Chem. Phys.* **1993**, *98*, 5648.